Supporting Information

Cr^{3+} based nanocrystalline luminescent thermometers operating in a temporal domain

*Karolina Elzbieciak-Piecka[1], Joanna Drabik[1], Daniel Jaque[2] and Lukasz Marciniak[1]**

[1]Institute of Low Temperature and Structure Research PAS, Wroclaw, Poland

[2]Universidad Autonoma de Madrid, Madrid, Spain

corresponding author: l.marciniak@intibs.pl

Keywords: Cr^{3+} luminescence decay times, lifetime based thermometry, methods of luminescence lifetimes determination

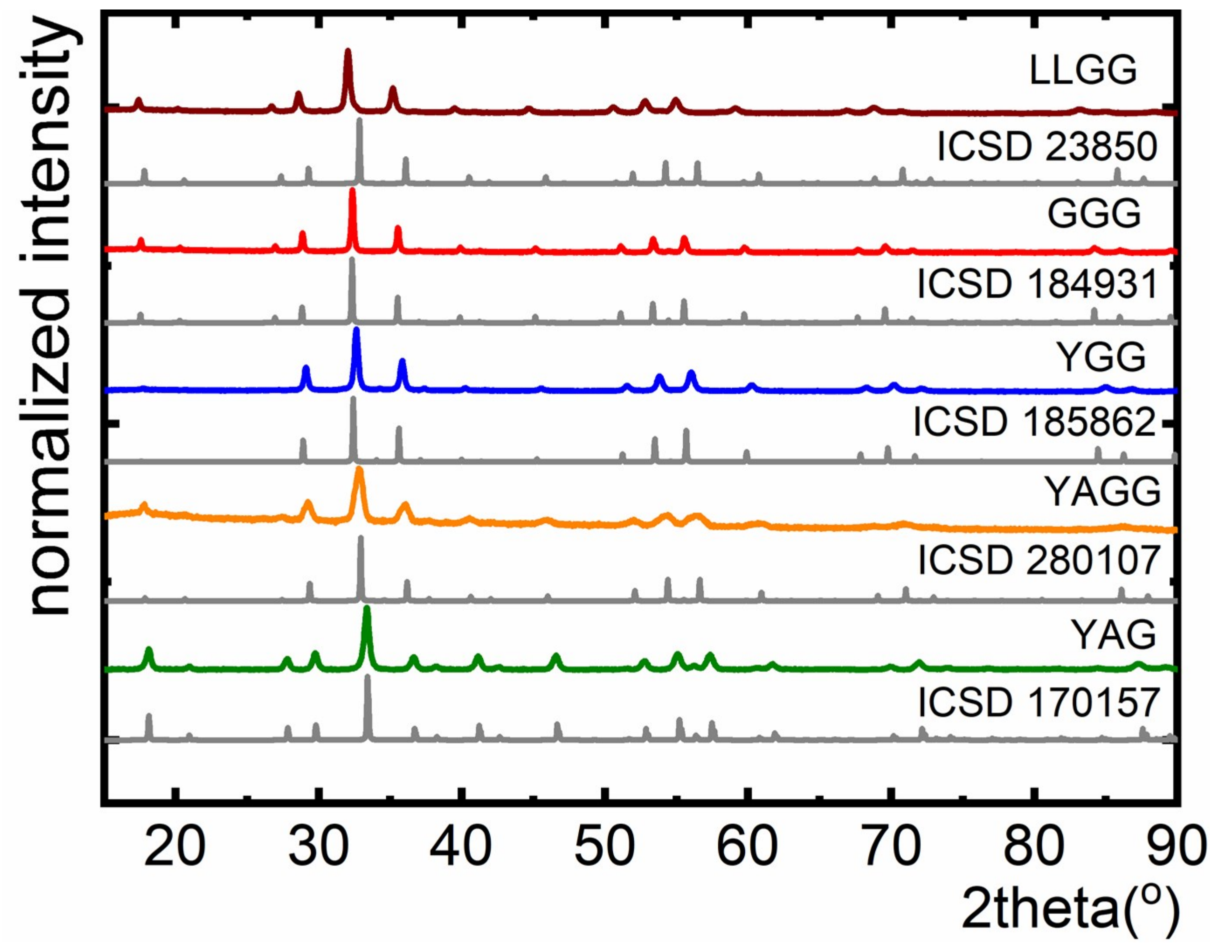

Figure S1. XRD patterns for $Y_3Al_5O_{12}$:2%Cr^{3+} (YAG), $Y_3Al_2Ga_3O_{12}$:2%Cr^{3+} (YAGG), $Y_3Ga_5O_{12}$:2%Cr^{3+} (YGG), $Gd_3Ga_5O_{12}$:2%Cr^{3+} (GGG) and $La_2LuGa_5O_{12}$:2%Cr^{3+} (LLGG) with corresponding reference patterns from ICSD.

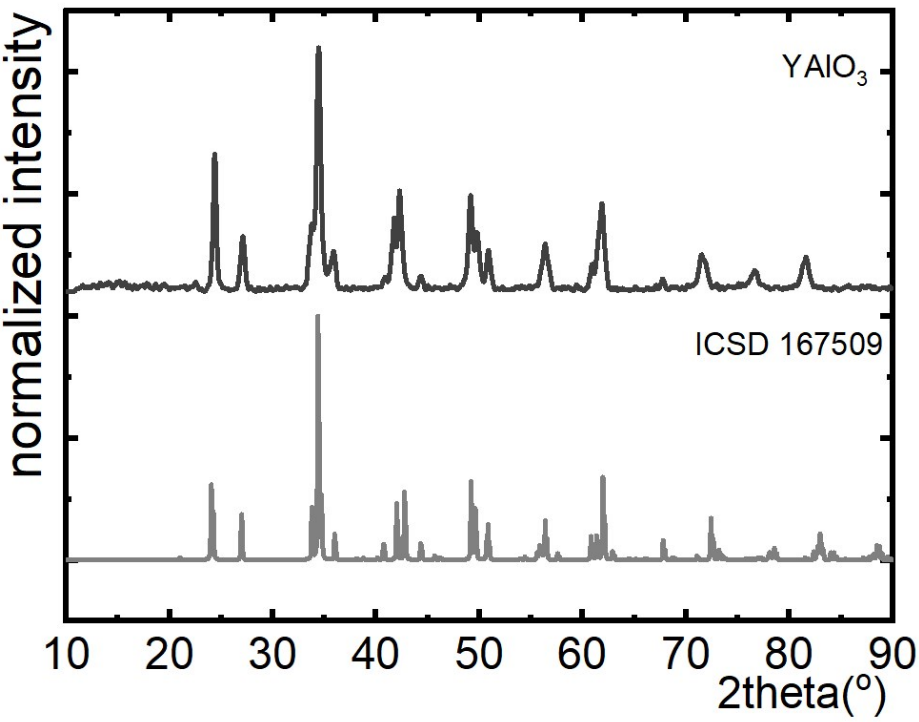

Figure S2. XRD patterns for $YAlO_3$: 2%Cr^{3+} (YAP) with reference from ICSD.

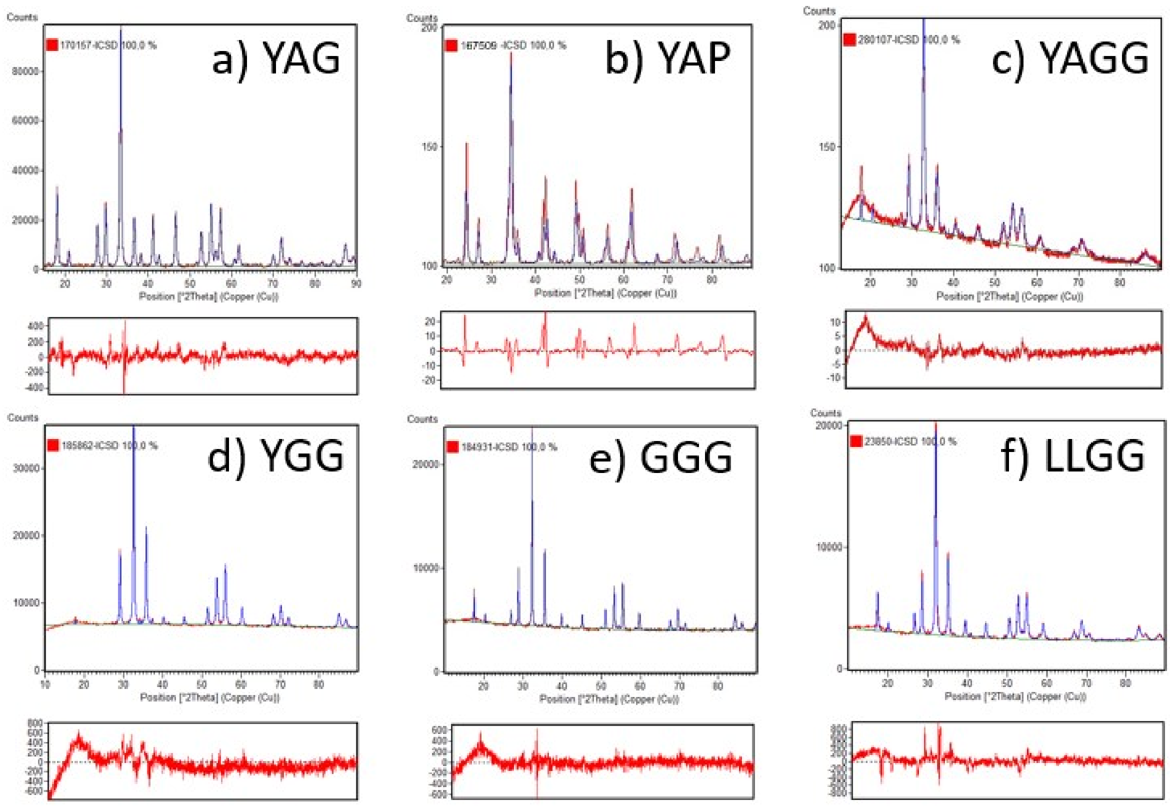

Figure S3. Rietveld refinement profiles of synthesized phosphors: YAG-a); YAP-b); YAGG-c); YGG-d); GGG-e) and LLGG-f).

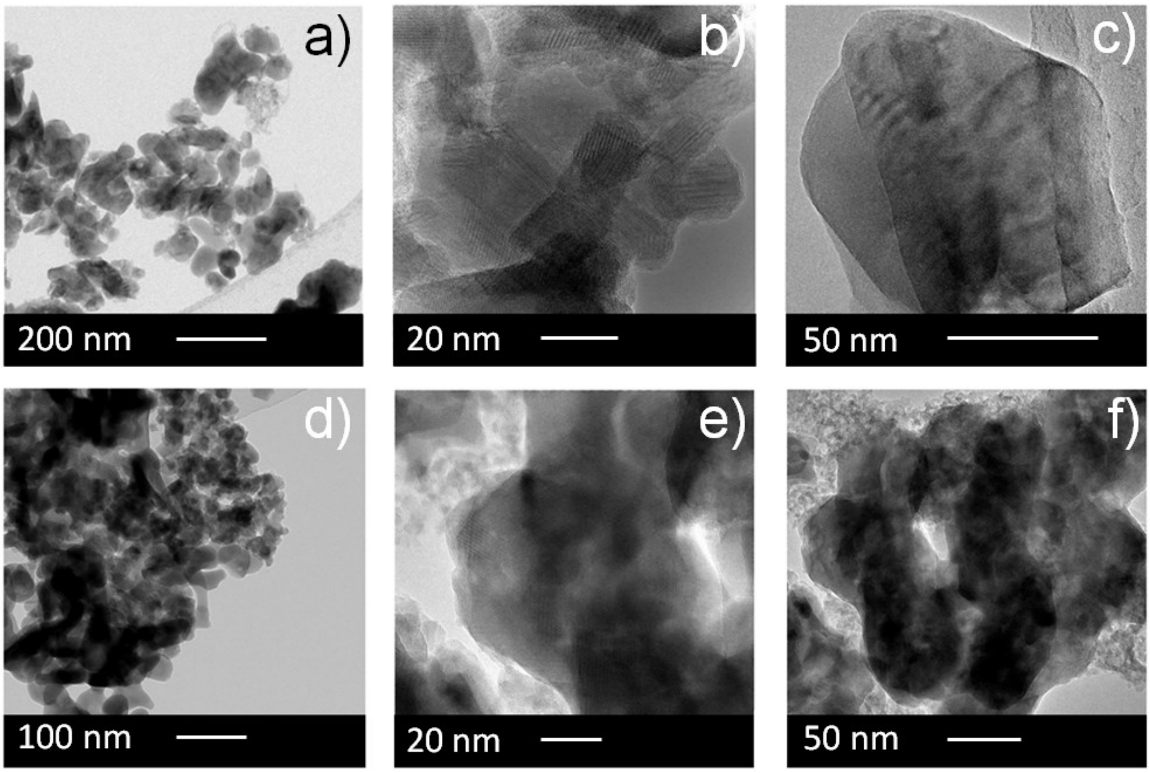

Figure S4. Representative TEM images for: YAGG-a,b), GGG-c), YGG-d) and YAG-e,f).

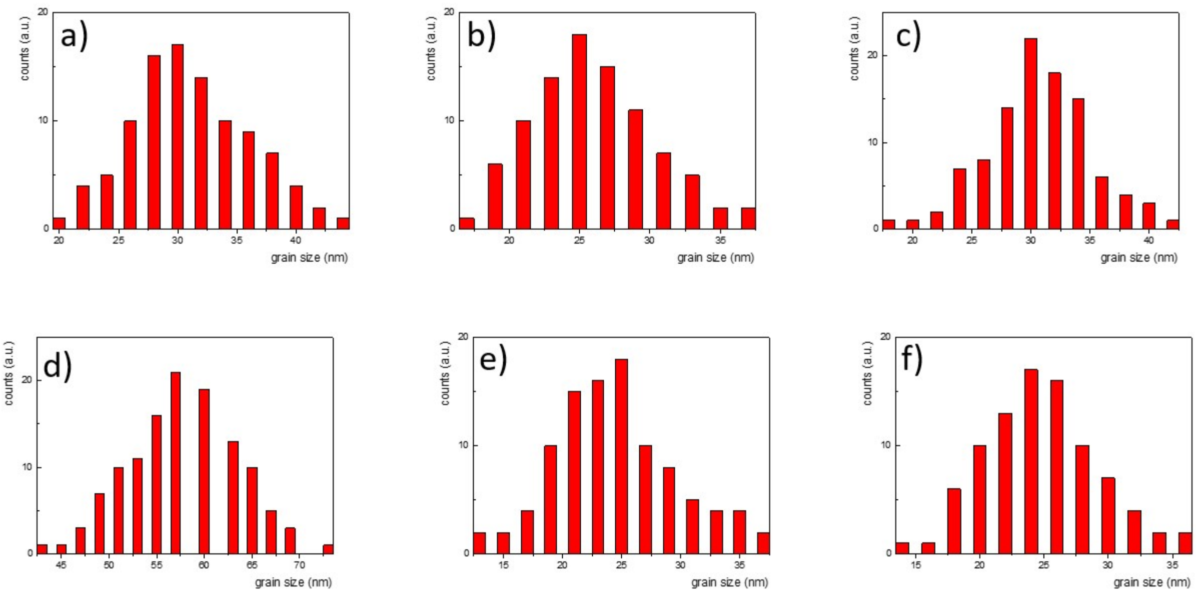

Figure S5. Histograms of the nanoparticle size distribution calculated based on TEM images for: YAG-a); YAGG-b); YGG-c); GGG-d); LLGG-e) and YAP –f).

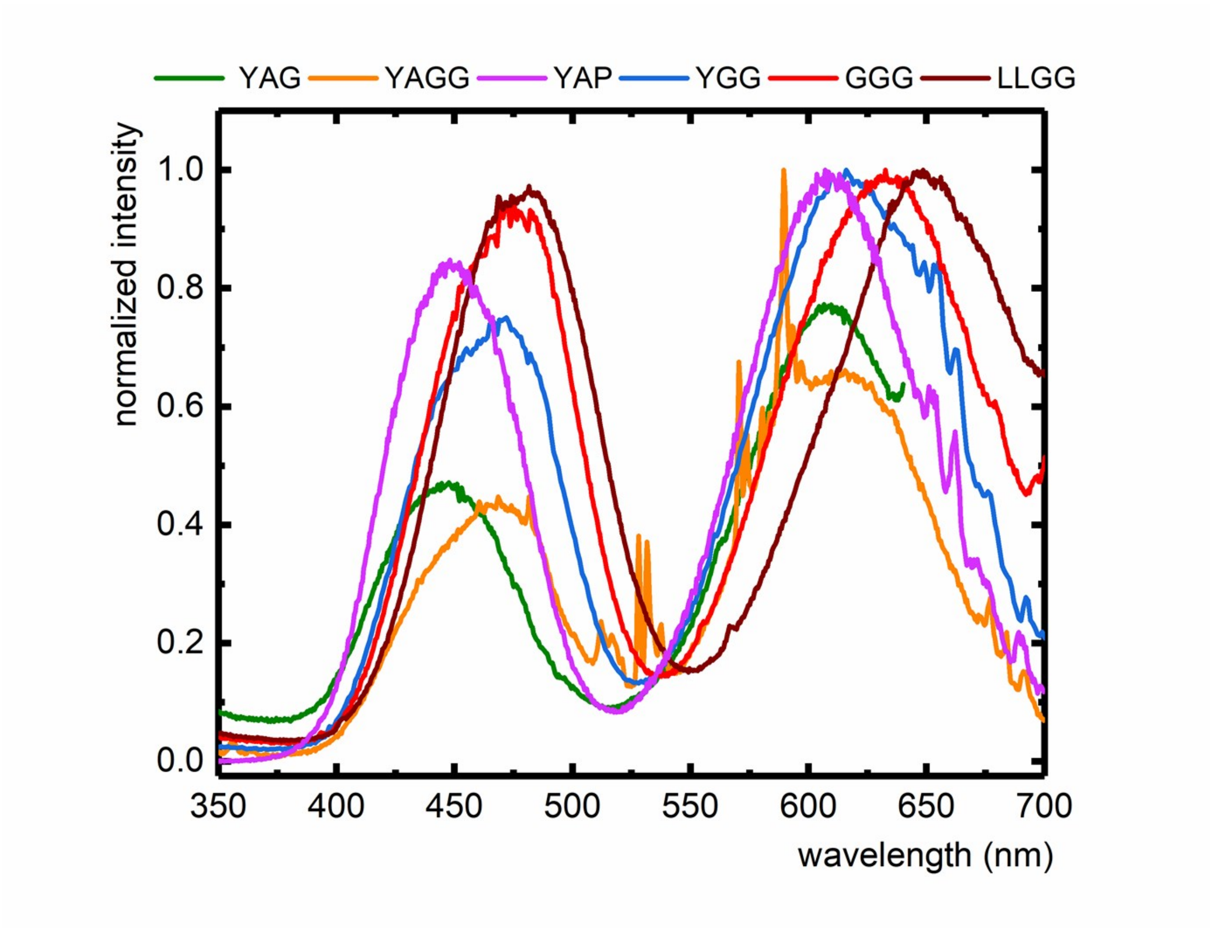

Figure S6. Comparison of excitation spectra for all investigated nanocrystals measured at RT with emission monitored at 720nm (YAG, YAP, YGG), 712nm (GGG) and 730nm (LLGG).

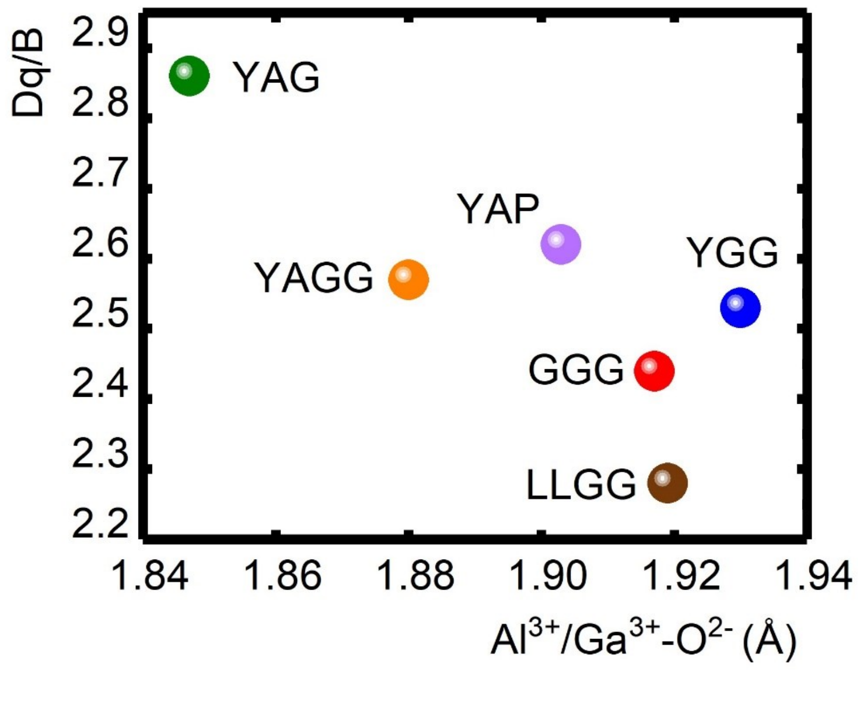

Figure S7. Correlation between crystal field strength parameter Dq/B and average metal-oxygen distance ($Al^{3+}/Ga^{3+}-O^{2-}$) all investigated nanocrystalline particles.

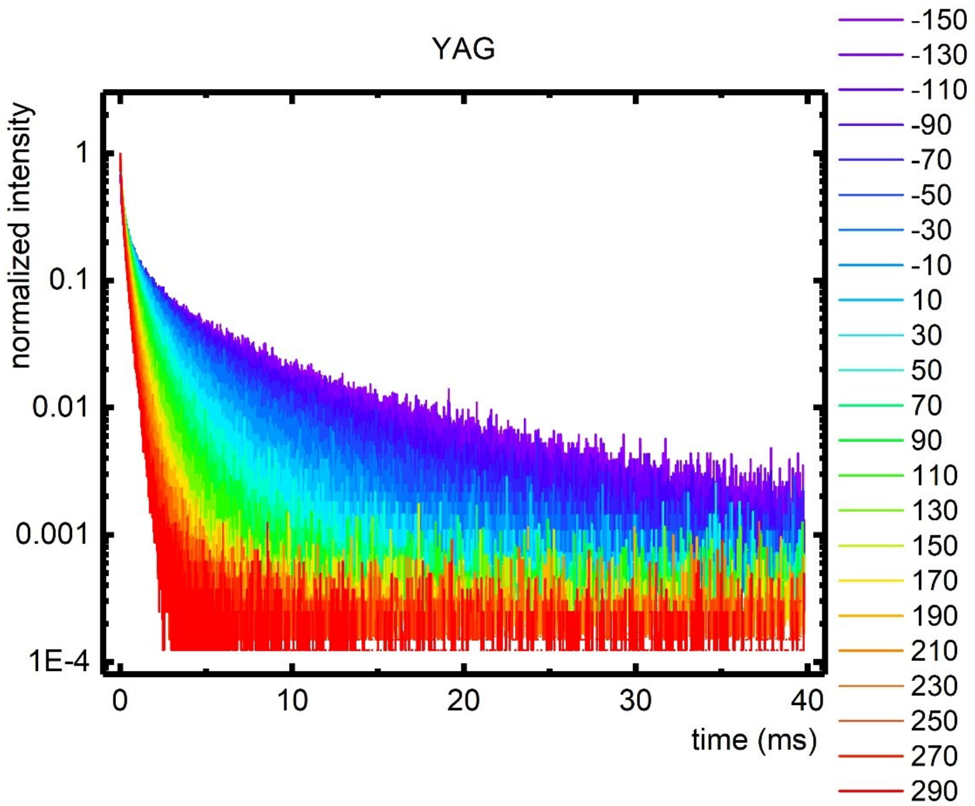

Figure S8. Thermal evolution of luminescence decay profiles of YAG (excited at 445nm with emission monitored at 720nm).

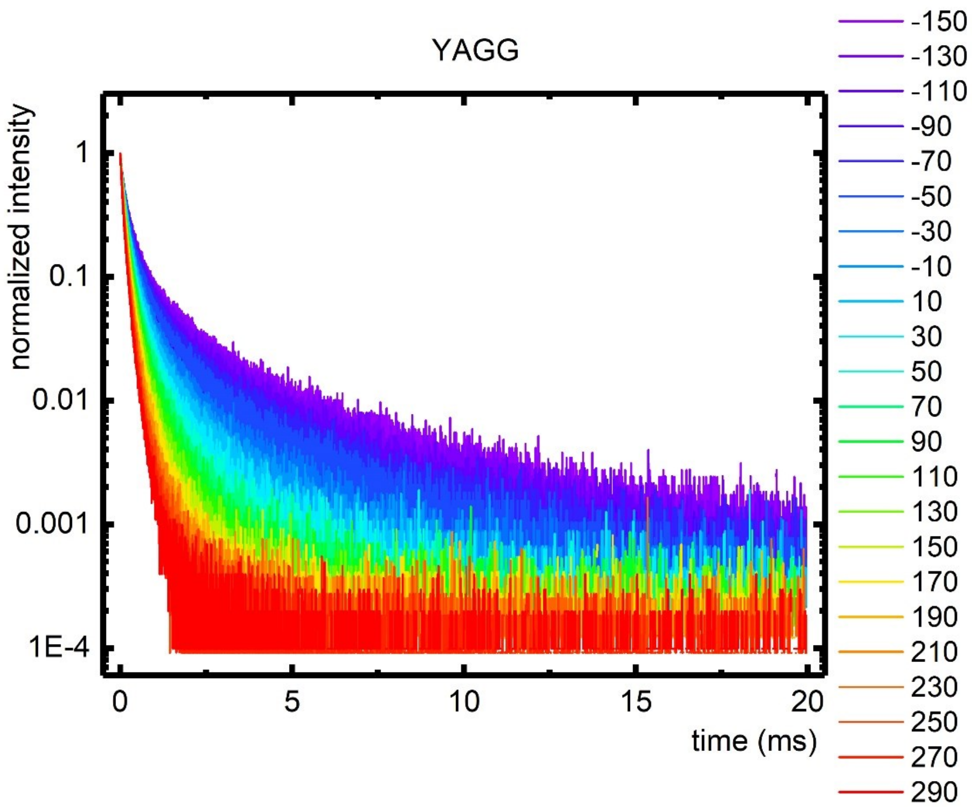

Figure S9. Thermal evolution of luminescence decay profiles of YAGG (excited at 445nm with emission monitored at 720nm).

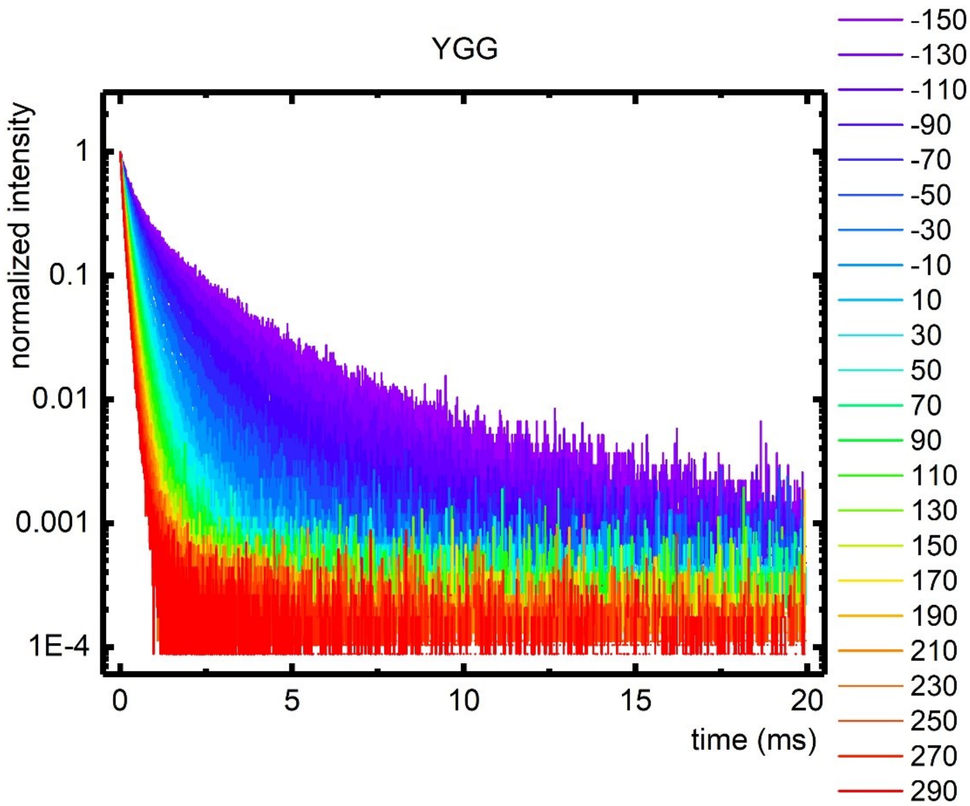

Figure S10. Thermal evolution of luminescence decay profiles of YGG (excited at 445nm with emission monitored at 720nm).

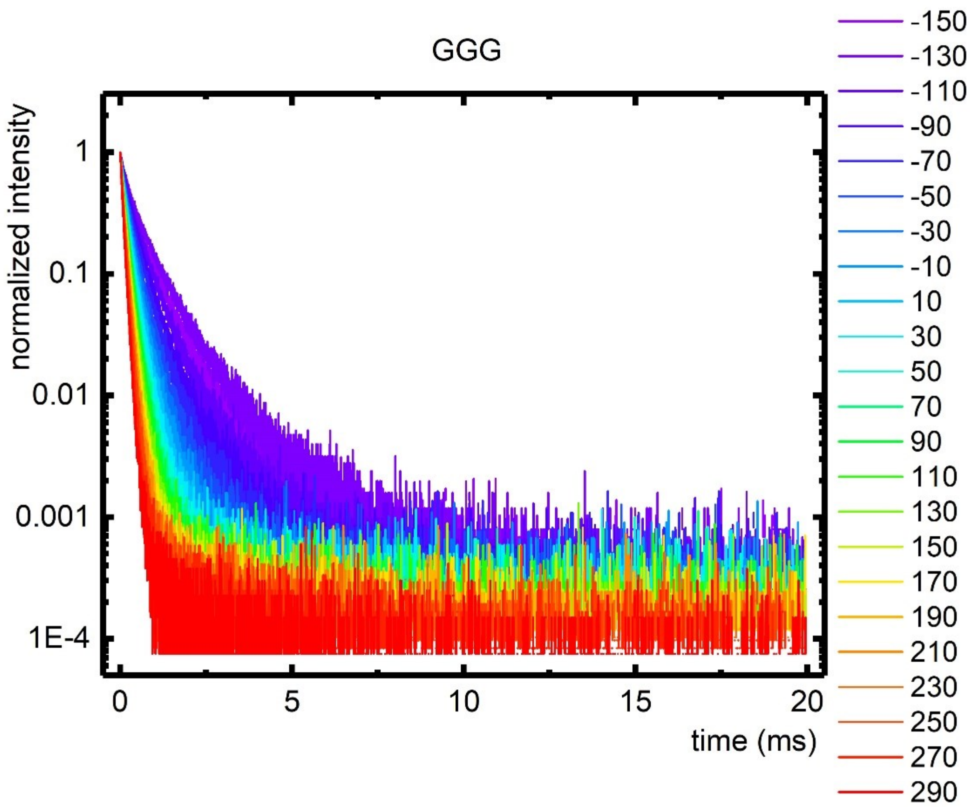

Figure S11. Thermal evolution of luminescence decay profiles of GGG (excited at 445nm with emission monitored at 720nm).

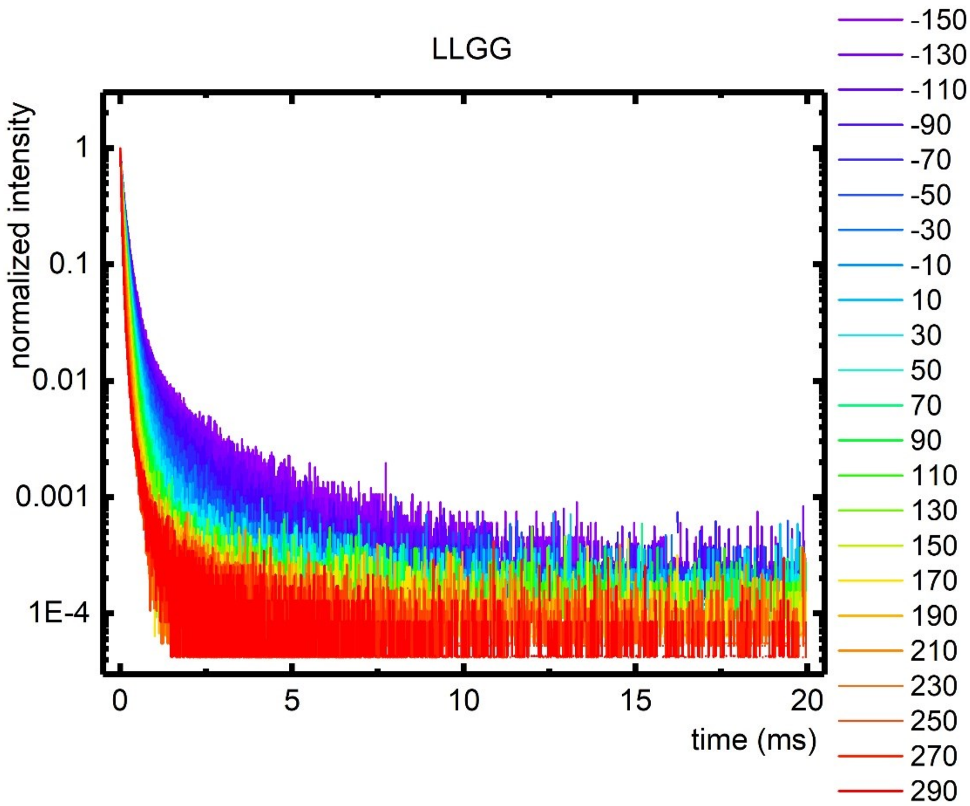

Figure S12. Thermal evolution of luminescence decay profiles of LLGG (excited at 445nm with emission monitored at 720nm).

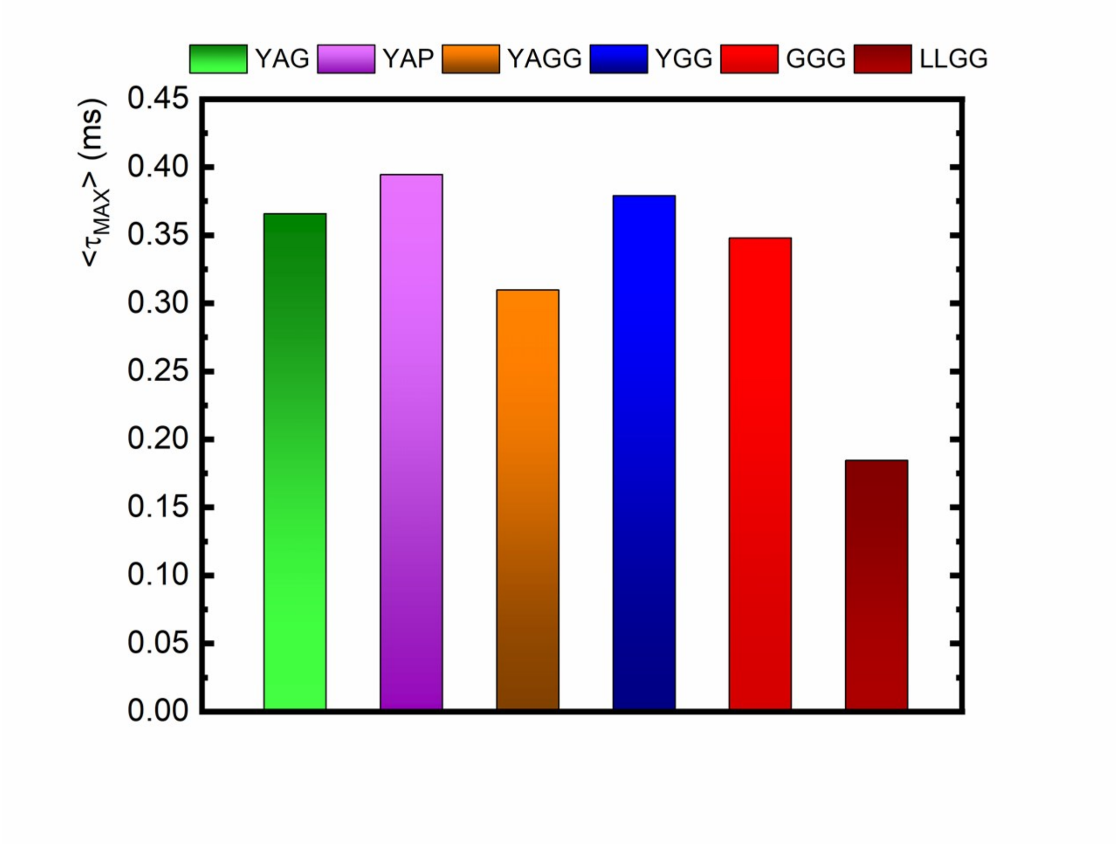

Figure S13. Maximal average luminescence lifetimes at -150°C arranged in the function of lowering Dq/B parameter.

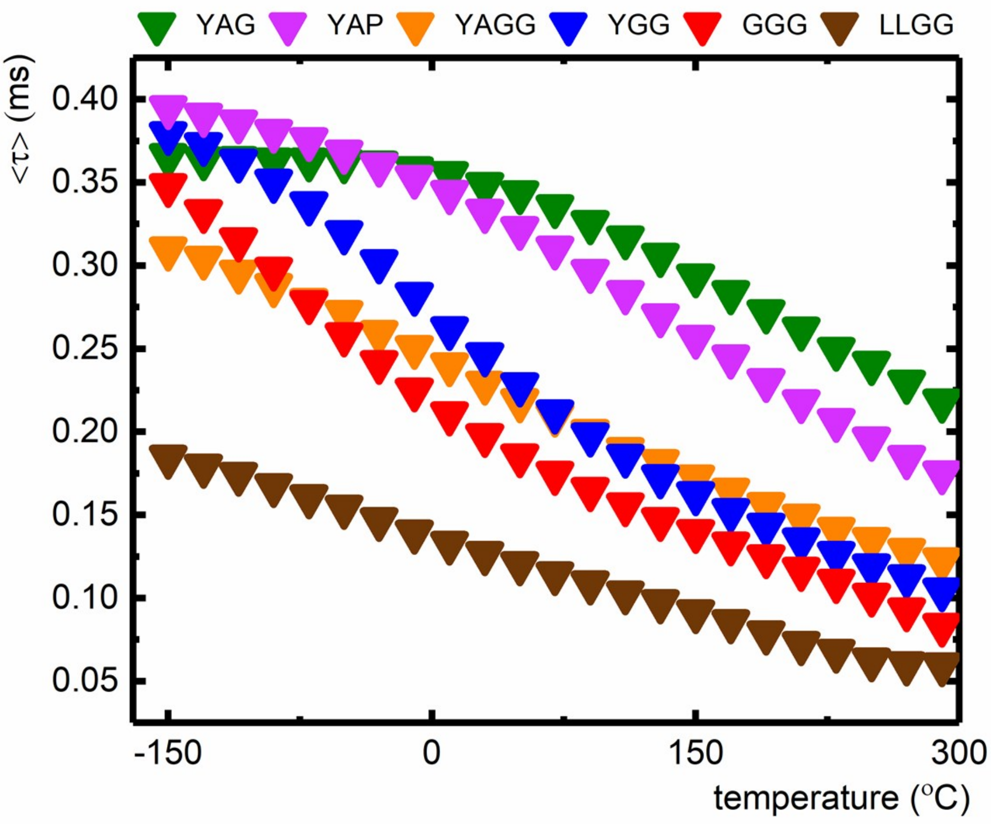

Figure S14. Average luminescence lifetimes for all investigated materials in the function of temperature.

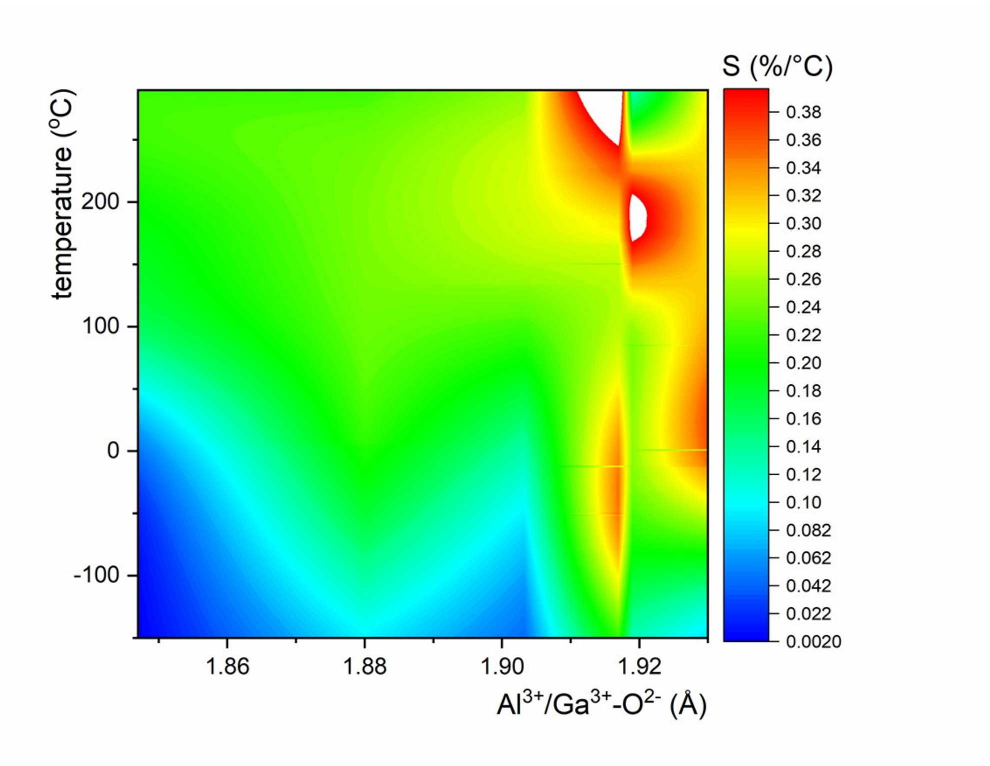

Figure S15. Sensitivity map for ALA as a function of Al^{3+}/Ga^{3+}-O^{2-} ionic distances and temperature.

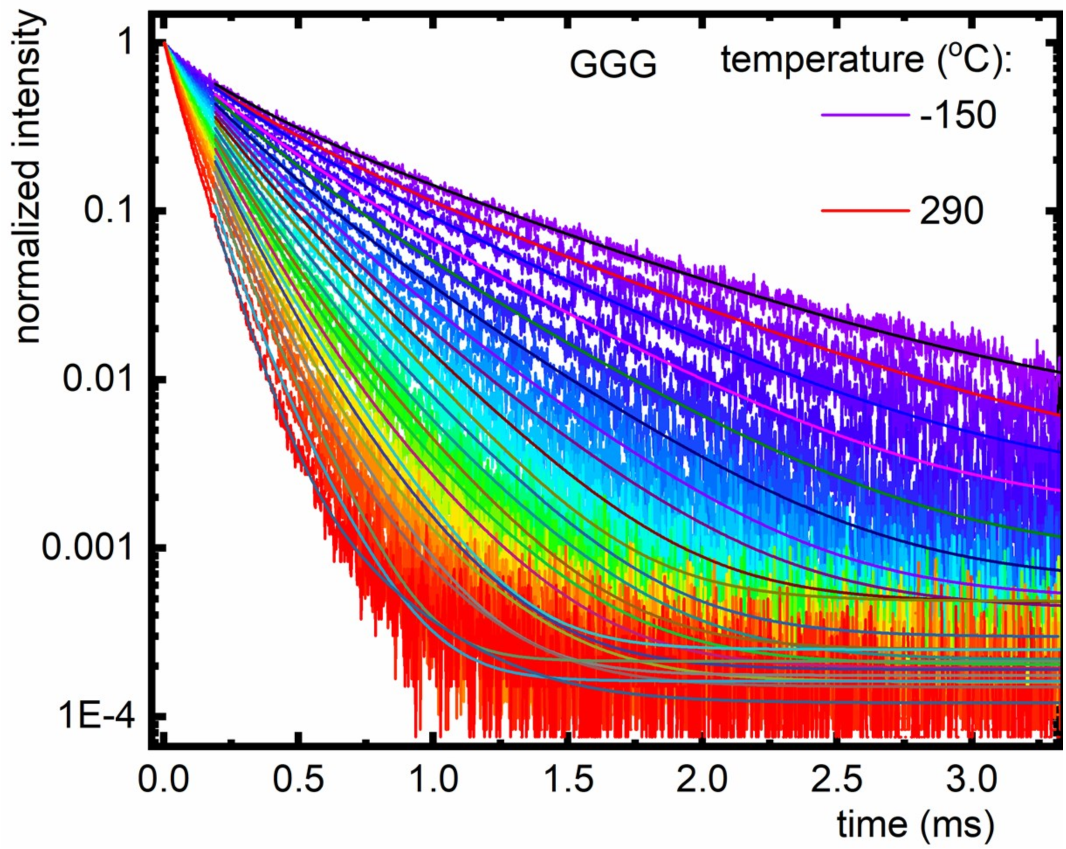

Figure S16. Decay profiles obtained at different temperatures for GGG fitted with double exponential function

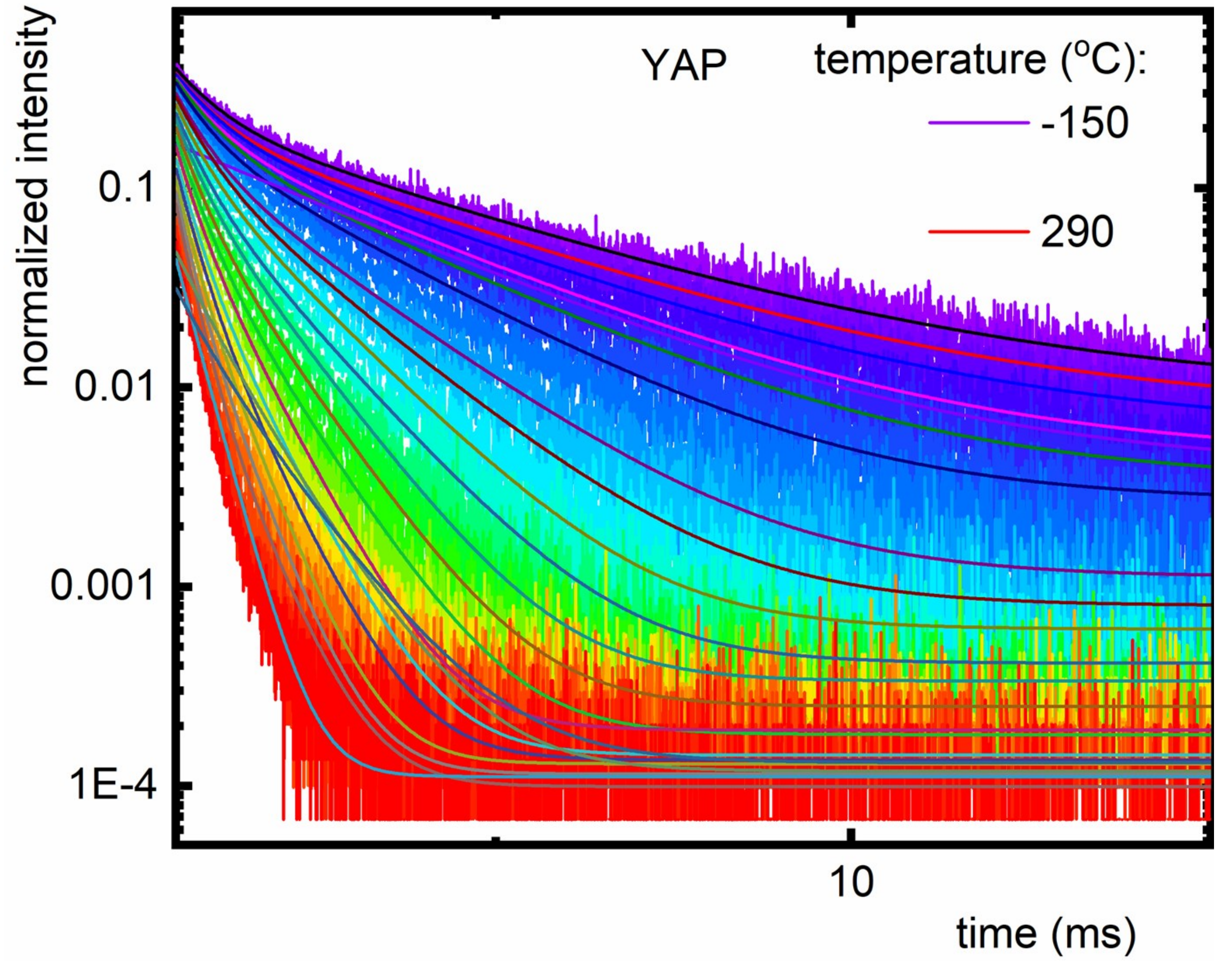

Figure S17. Decay profiles obtained at different temperatures for YAP fitted with double exponential function

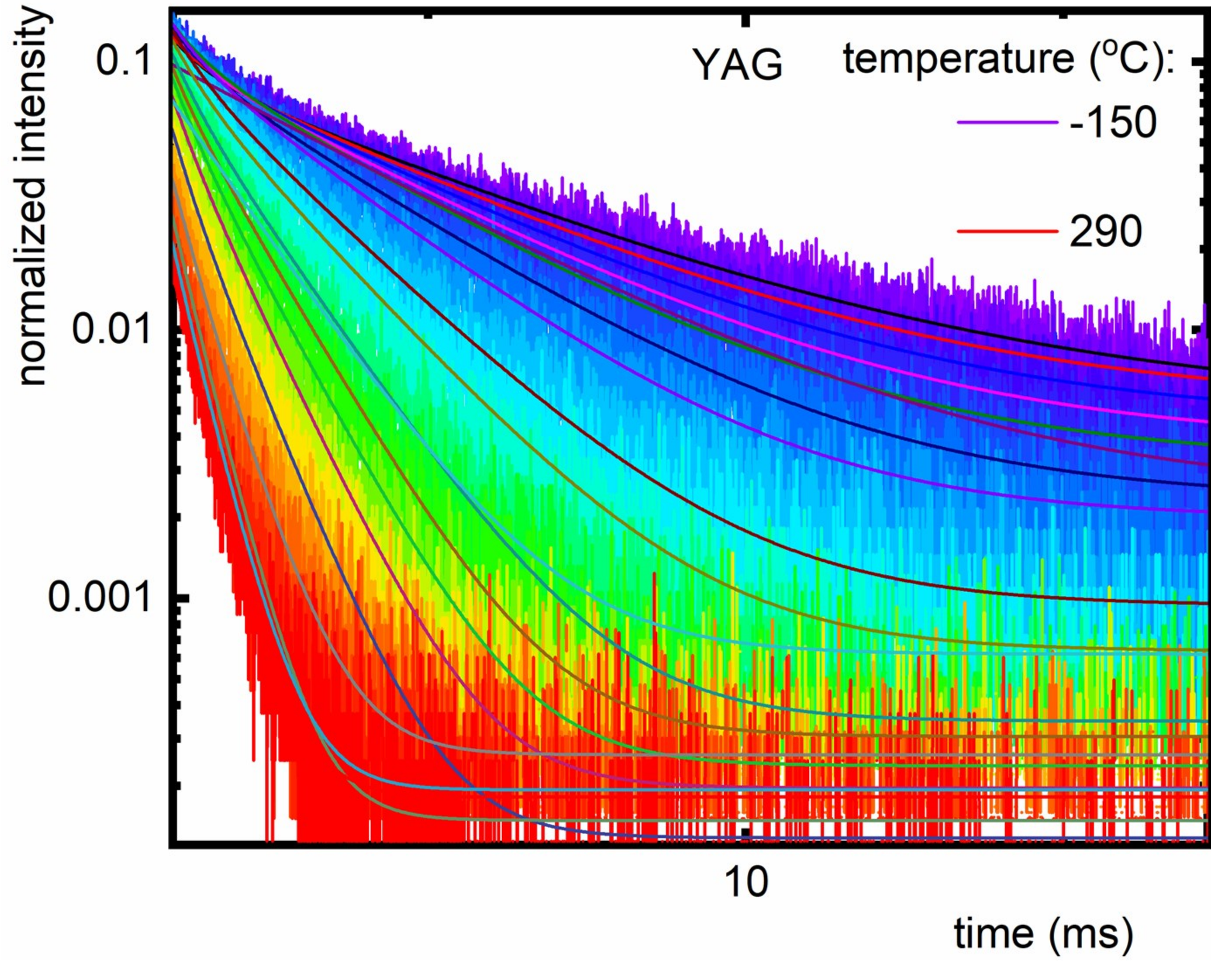

Figure S18. Decay profiles obtained at different temperatures for YAG fitted with double exponential function

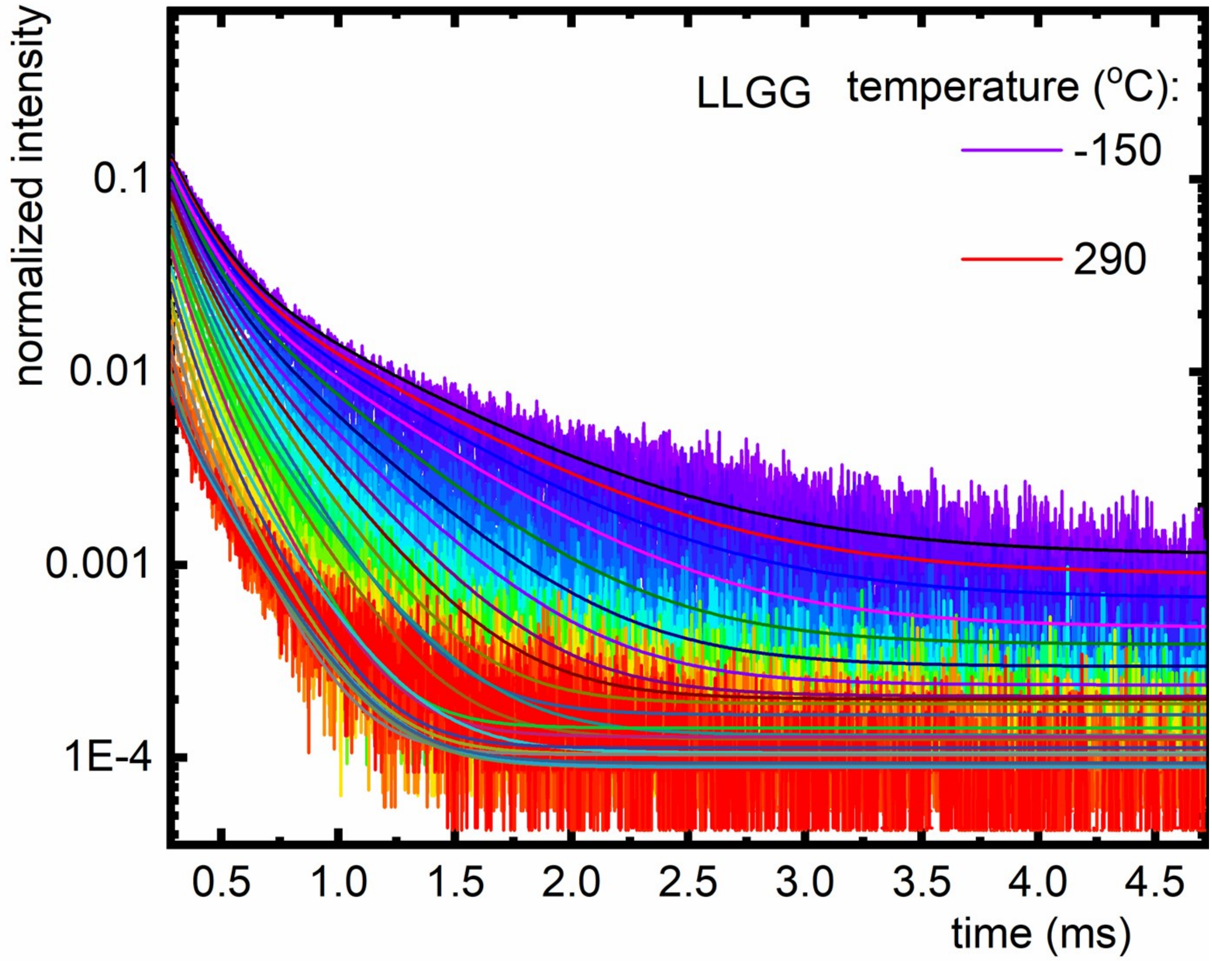

Figure S19. Decay profiles obtained at different temperatures for LLGG fitted with double exponential function

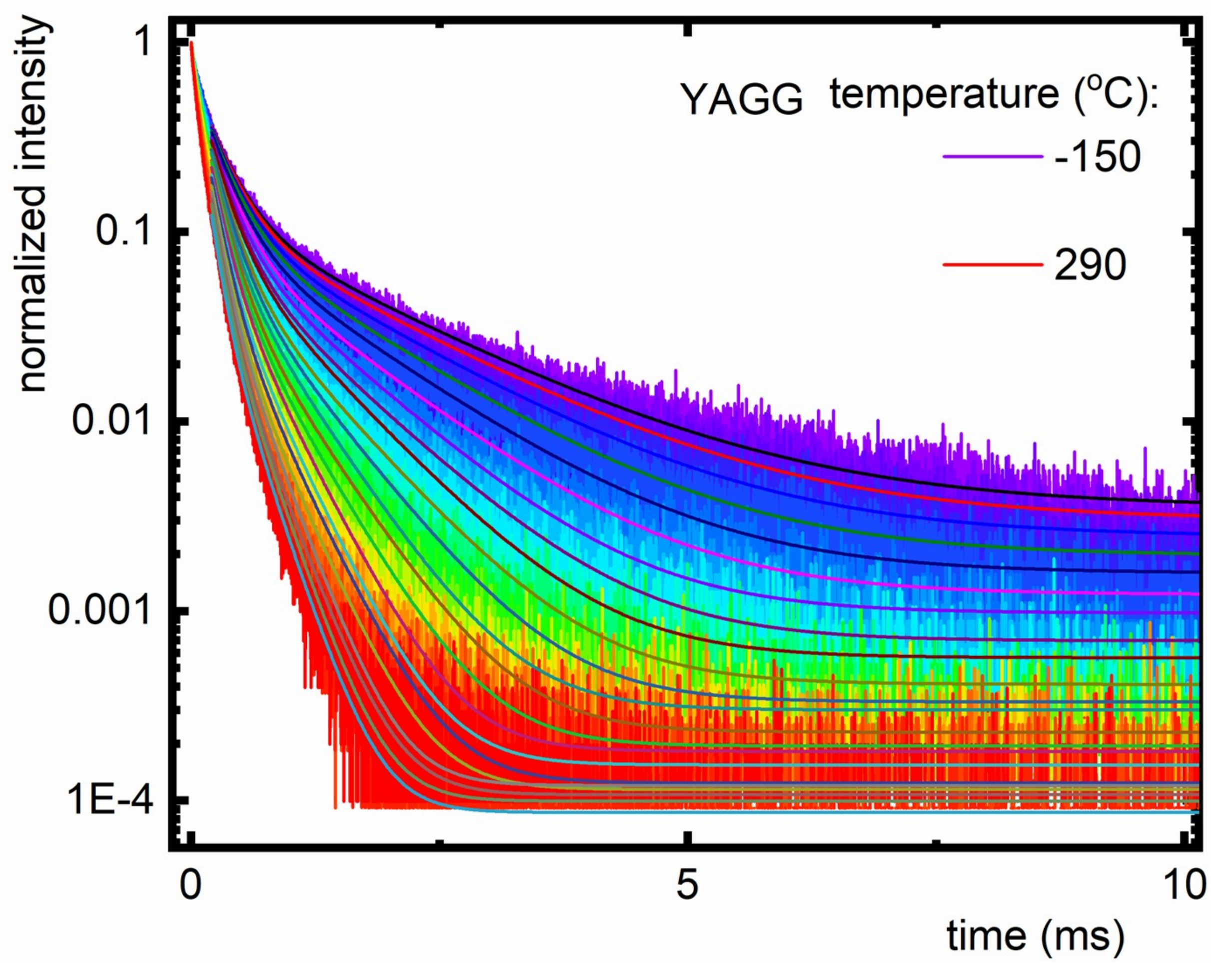

Figure S20. Decay profiles obtained at different temperatures for YAGG fitted with double exponential function

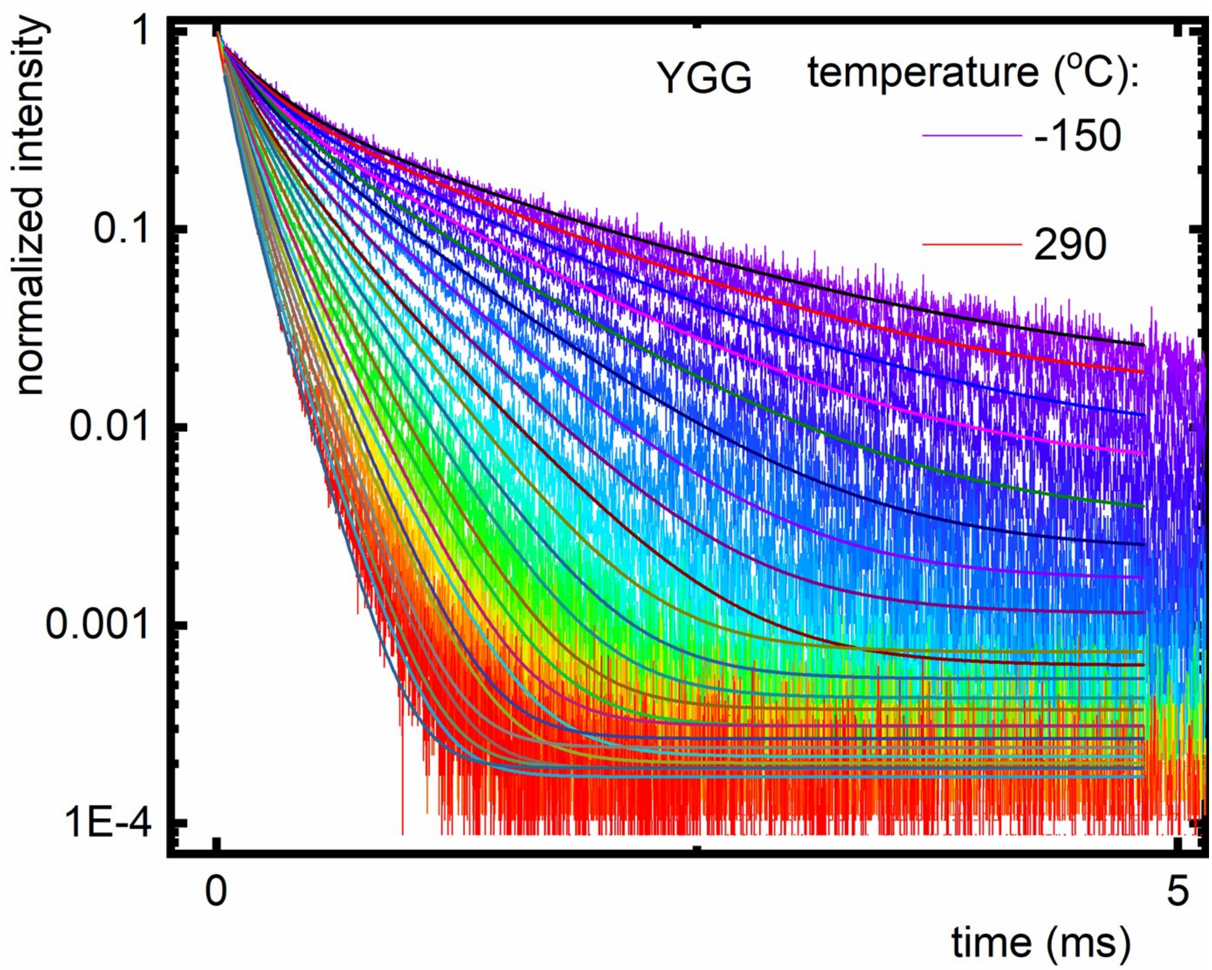

Figure S21. Decay profiles obtained at different temperatures for YGG fitted with double exponential function

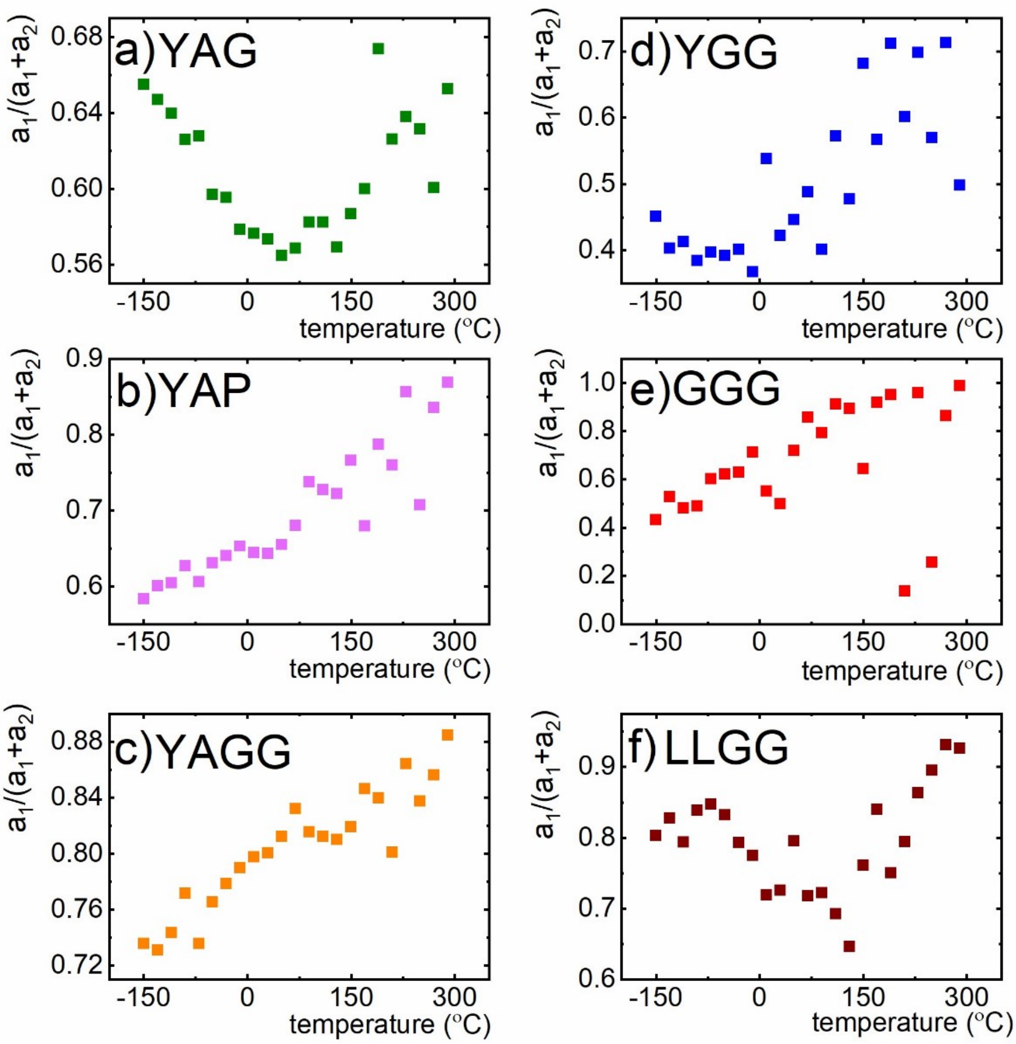

Figure S22. The contribution of the amplitude a_1 to the sum of the amplitudes (a_1+a_2) as a function of temperature for YAG –a), YAP –b), YAGG –c), YGG –d), GGG –e) and LLGG –f) obtained from double exponential fit.

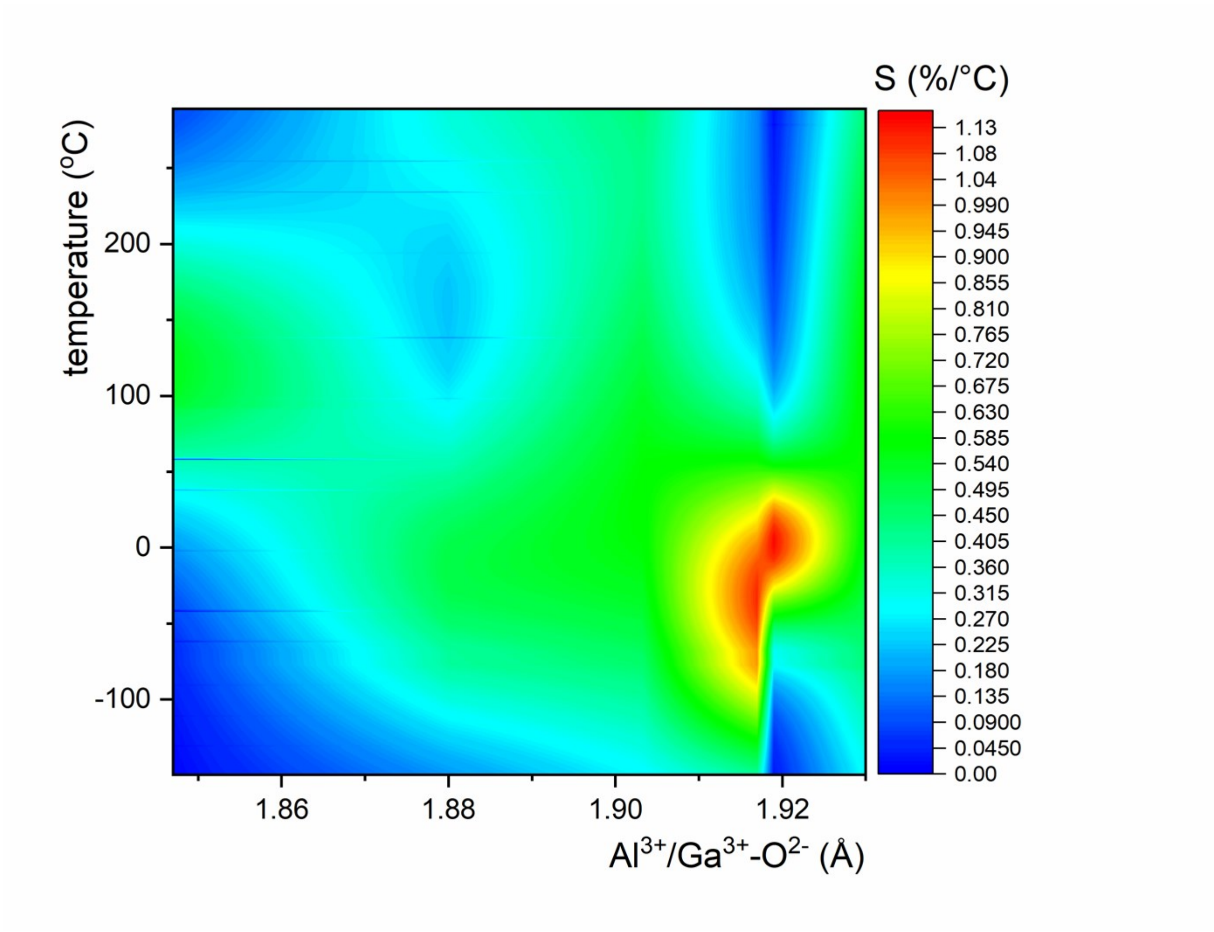

Figure S23. Sensitivity map for W parameter as a function of Al^{3+}/Ga^{3+}-O^{2-} ionic distances and temperature.

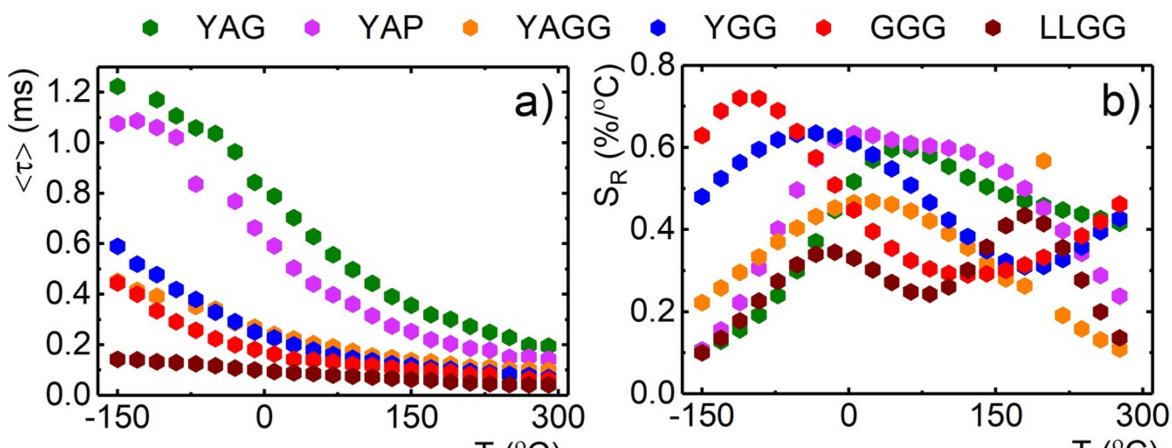

Figure S24. Thermal evolution of the average lifetime calculated using eq. 8-a) and the corresponding S_R-b).

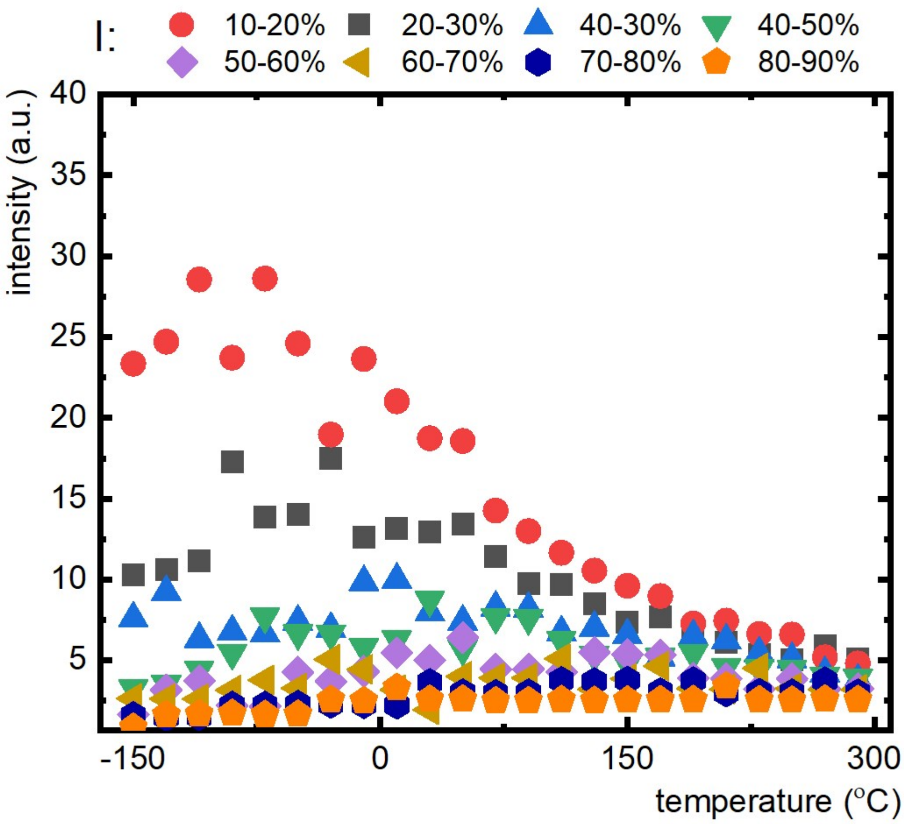

Figure 25. Thermal evolution of the intensity signal calculated for different intensity-based ranges for representative nanocrystals YAG:Cr^{3+}

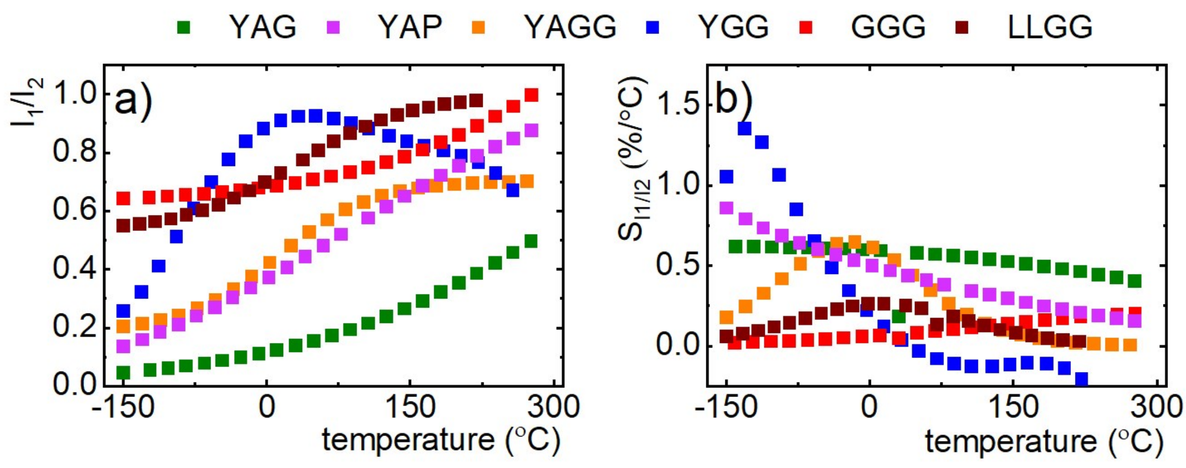

Figure 26. Thermal evolution of the I_1/I_2 emission intensity ratio –a) and the corresponding SR-b for I-TGRA method.

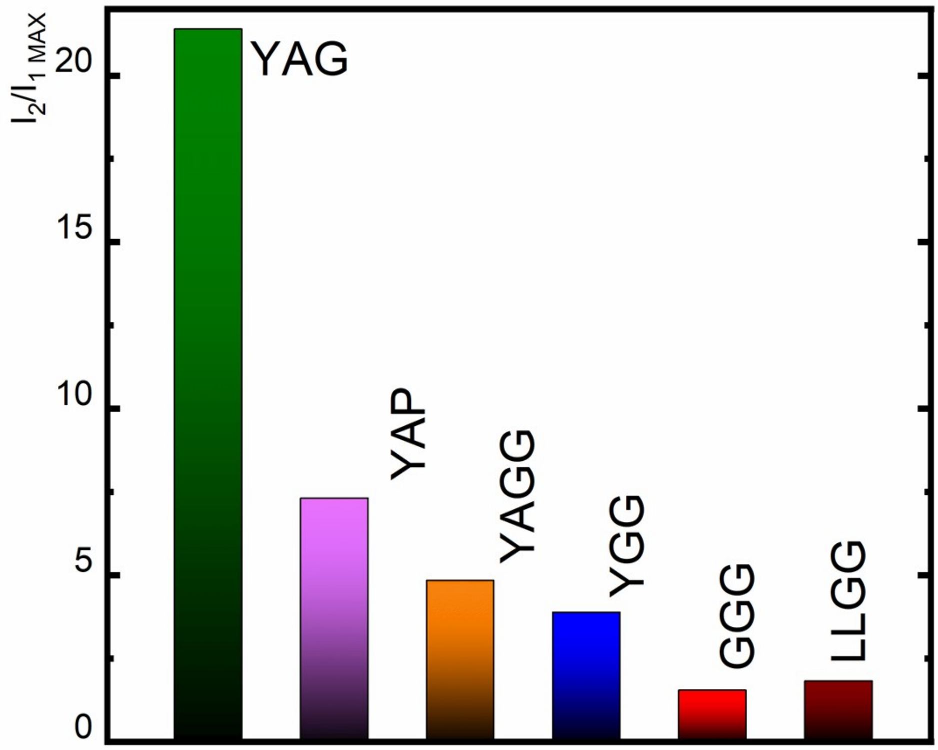

Figure S27. Maximal values of I_2/I_1 ratio for I-TGRA arranged in the function of lowering Dq/B parameter.